AFRL-AFOSR-UK-TR-2011-0034

Numerical Simulation of Ultra-Fast Pulse Propagation in Two-Photon Absorbing Medium

Raivo Stern
Aleks Rebane

National Institute of Chemical Physics and Biophysics (NICPB)
Keemilise ja Bioloogilise Fuusika Instituut
Akadeemia Tee 23
Tallinn, Estonia 12618

EOARD GRANT 10-3071

August 2011

Final Report for 16 June 2010 to 16 June 2011

Air Force Research Laboratory
Air Force Office of Scientific Research
European Office of Aerospace Research and Development
Unit 4515 Box 14, APO AE 09421

REPORT DOCUMENTATION PAGE

Form Approved OMB No. 0704-0188

1. REPORT DATE *(DD-MM-YYYY)*	2. REPORT TYPE	3. DATES COVERED *(From – To)*
09-08-2011	Final Report	16 June 2010 – 16 June 2011

4. TITLE AND SUBTITLE

Numerical Simulation of Ultra-Fast Pulse Propagation in Two-Photon Absorbing Medium

5a. CONTRACT NUMBER

FA8655-10-1-3071

5b. GRANT NUMBER

Grant 10-3071

5c. PROGRAM ELEMENT NUMBER

6. AUTHOR(S)

Raivo Stern
Aleks Rebane

5d. PROJECT NUMBER

5d. TASK NUMBER

5e. WORK UNIT NUMBER

7. PERFORMING ORGANIZATION NAME(S) AND ADDRESS(ES)

National Institute of Chemical Physics and Biophysics (NICPB)
Keemilise ja Bioloogilise Fuusika Instituut
Akadeemia Tee 23
Tallinn, Estonia 12618

8. PERFORMING ORGANIZATION REPORT NUMBER

N/A

9. SPONSORING/MONITORING AGENCY NAME(S) AND ADDRESS(ES)

EOARD
Unit 4515 BOX 14
APO AE 09421

10. SPONSOR/MONITOR'S ACRONYM(S)

AFRL/AFOSR/RSW (EOARD)

11. SPONSOR/MONITOR'S REPORT NUMBER(S)

AFRL-AFOSR-UK-TR-2011-0034

12. DISTRIBUTION/AVAILABILITY STATEMENT

Approved for public release; distribution is unlimited. (approval given by local Public Affairs Office)

13. SUPPLEMENTARY NOTES

14. ABSTRACT

Developed a versatile numerical technique that allows us to calculate the energy, the temporal shape, the spectrum and the phase of an ultrashort pulse propagating in multi-photon absorbing medium with fully realistic spectral shapes and absorption profiles. This approach is based on solving straightforward ODE instead of Maxwell-Bloch type equations, which usually require FTDT calculations. Furthermore, the solver is implemented using 100% commercial software (*Mathematica* ver. 8) running on a conventional multi-core PC platform, which avoids complications and increased costs associated with need for custom-produced code and/or large-scale computing facilities. This fact in itself is quite remarkable, especially because we were solving a set of stochastic equations that required extensive averaging. First, verifying the accuracy of the calculation by comparing to some simple analytical formulas and demonstrate its utility by analyzing the optical power limiting performance of a known two-photon organic chromophore. Also, show that the calculation yields full information about the amplitude and phase of the pulse.
Looking forward, we envision the new solver can be applied for the simulation and analysis of a broad range of physical problems including coherent- and incoherent regimes of optical power limiting, saturation, CEP effects, soliton formation etc. It can be also used for optimization of Materials that are used in multi-photon microscopy and imaging.

15. SUBJECT TERMS

EOARD, Non-linear Optical Materials , ultrashort pulse interactions

16. SECURITY CLASSIFICATION OF:			17. LIMITATION OF ABSTRACT	18, NUMBER OF PAGES	19a. NAME OF RESPONSIBLE PERSON
a. REPORT	b. ABSTRACT	c. THIS PAGE			A. GAVRIELIDES
UNCLAS	UNCLAS	UNCLAS	SAR	23	19b. TELEPHONE NUMBER *(Include area code)* +44 (0)1895 616205

AFOSR Award Nr. FA8655-10-1-3071

European Office of Aerospace Research and Development EOARD

Numerical Simulation of Ultra-Fast Pulse Propagation in Two-Photon Absorbing Medium

Project Start Date 16 June 2010
Final Technical Report 30 July 2011

Raivo Stern

Aleks Rebane

National Institute of Chemical Physics and Biophysics, Tallinn, Estonia

Keemilise ja Bioloogilise Füüsika Instituut

Akadeemia Tee 23, Tallinn 12618, Estonia

Phone: +372-5132288

Email:stern@kbfi.ee raivo.stern@gmail.com

Table of content

1. Summary

We have developed a new numerical solver that models propagation of femtosecond pulses in multi-photon absorbing media. The *Mathematica*-based numerical calculation predicts how transmission through a medium comprising two-photon absorbing (2PA) chromophores at a given concentration and with given molecular parameters changes the energy, the temporal- and spectral amplitude and the phase of the pulse. Our formalism makes use of full three-level stochastic density matrix (SDM) equations of motion, which allows us to study optical power limiting medium in a broad range of parameters, including the coherent regime of the light-matter interaction, i.e. when the duration of the pulse is comparable or shorter that the decoherence time of the medium. Furthermore, because the SDM equations allow modeling of arbitrary non-Loretzian line shapes, our calculation takes into account the realistic resonance line shape, including both one-photon and two-photon spectra of the chromophore.

We apply the new numerical solver to 100-fs Gaussian pulse of variable peak intensity $10\text{-}10^3$ GW cm^2. The pulse is incident on two-level or three-level medium where the molecular parameters, including the transition frequencies, the values of the transition electric dipole moments and the difference between the permanent electric dipole moments are modeled after a well-known 2PA chromophore trans-4,4'-Bis(diphenylamino)stilbene (BDPAS). Modeling of most other 2PA chromophores is readily feasible by appropriate change of the parameters. With the goal of validating our calculation we verify that at moderate intensity $<10^2$ GW cm^2 the numerical results are quantitatively in agreement with the analytical solution. We calculate the transmission of 100-fs pulse through BDPAS medium at chromophore concentration $0.5\ 10^{19}$ cm^{-3} and show that the minimum propagation distance for the optical power limiting to take effect is about 0.4 cm and that larger distance >0.5 cm is needed for incident intensity $>3\ 10^3$ GW cm^{-2} due to saturation of the 2PA. At the same time, the temporal shape of the transmitted pulse changes from flat-topping at moderate intensity to an asymmetrical shape at high intensity, whereas the spectral maximum shifts to higher frequency. These results agree with earlier experimental observations in quantum-dot-doped waveguides. Finally, we calculate few-cycle 5-fs pulse propagating in dipolar two-level medium and show that the shape changes depending on the carrier-envelope phase (CEP) of the incident pulse.

We envisage that the solver can be applied for simulation of a broad range of physical problems including coherent- and incoherent regimes of optical power limiting, saturation, CEP effects, electromagnetically induced transparency, soliton formation etc.

2. Introduction

Interaction of high peak intensity light pulses with a multi-photon absorbing medium is an important issue in a number of ultrafast photonics applications. Developing a practical yet accurate numerical tool for modeling of the propagation of a femtosecond laser pulse in a two-photon absorbing (2PA) media would benefit optimization of optical power limiting devices, all-optical switches, two-photon fluorescence microscopes etc.

In this project we have developed a *Mathematica*-based numerical calculation that simulates how the energy, temporal- and spectral amplitude and phase of a femtosecond pulse develops as the pulse propagates in a medium comprising two-photon absorbing chromophores. We use density matrix equation formalism, which allows us to study the transmission through an optical power limiting medium in coherent regime, where the duration of the pulse is comparable or shorter that the decoherence time of the medium. The new numerical ultrafast pulse propagation solver allows us to calculate the temporal- and spectral shape of the pulse as a function of key molecular parameters, such as transition frequency, values of the transition dipole moments and difference of the permanent electric dipole moments between different states, as well as the rates of decoherence and energy relaxation between the states. Furthermore, our model also allows taking into account realistic resonance line shapes of both one-photon and multi-photon transitions. We demonstrate the utility of our numerical algorithm by modeling the optical power limiting performance of a medium comprising known organic chromophore and comparing our results to analytical solutions obtained in the limit where the role of coherent effects is minimal.

Most previous works addressing the modeling of pulse propagation in multi-photon optical power limiting medium rely on the circumstance that coherence of multi-photon optical transitions is typically rather short-lived, on the time scale of 100 fs or less. If the duration of the incident pulses is substantially longer than the decoherence time, then it is possible to assume that the 2PA process takes place practically instantaneously. This so-called "incoherent" description of the light-matter interaction is valid if the following two key conditions are satisfied: (i) the rate of the excitation of the 2PA transition remains relatively low compared to the rates of decoherence of the excited states and (ii) the bandwidth of the pulse is narrow compared to the spectral absorption features of the chromophore, including one-photon as well as multi-photon transitions. In this case the light pulse behaves essentially as monochromatic wave and the excitation processes in the optical limiting medium may be adequately described in terms of kinetic equations linking the population in different energy eigenstates with the rates of excitation and rates of energy relaxation. Due to relative simplicity of "incoherent" optical power limiting, this approach has been instrumental in analyzing the performance of NLO media from pico- to microsecond time scale, including those which take advantage of step-wise absorption from excited singlet- and triplet states [1-7].

In the project described here we are addressing what we call "coherent" regime of optical limiting, where the assumption of instantaneous transitions may no longer be valid. This regime is relevant in case of optical limiting media comprising organic chromophores will distinct electronic-vibrational spectral features and if the incident pulse has a high intensity, I_{in} >1-10^2 GW cm^{-2} and the duration of the pulse is 100 fs or less. In this case the ability of "incoherent" models to predict the energy of the transmitted pulse is rather limited because kinetic equations do not adequately describe the change of the temporal- and spectral shape of the pulse. In fact, if the 2PA is considered instantaneous, then this is equivalent to demanding that the attenuation of the intensity at any time is strictly proportional to the instantaneous intensity at that time. This means that the phase of the incident pulse has no influence on the optical power limiting, which is, of course, because the kinetic equations account only

for the intensity and not the phase. In order to take adequately into account coherent effects we use a more accurate photo-physical model that is based on solving density matrix (DM) equations of motion describing how the incident light interacts with the chromophores. Even though the solution of DM equations is computationally much more demanding than solution kinetic equations, this approach allows us to explicitly accounts for the temporal- and spectral phase of the pulse. Previously, Wang et al. [8] have solved numerically the Maxwell-Bloch DM equations using finite-difference time-domain (FDTD) technique to study the propagation of femtosecond laser pulses in strong two-photon absorption organic molecular medium. However, most likely due to inherent limitations of the finite-difference methods, their solutions were restricted to very short propagation distances less than 10 μm and extremely short pulses containing only a few oscillation cycles. Our calculation uses an alternative approach which permits, for the first time, the study of the spectral-, temporal and phase reshaping for much longer pulses containing up to hundreds of optical cycles and for arbitrary propagation length.

To achieve this objective we have combined the numerical solution of DM equations with a modified step-by-step description of the propagation in the forward direction. We have developed a *Mathematica*-based numerical code that allows, for the first time, accurate quantitative description of the temporal- and spectral shape of the pulse as it propagates in the 2PA medium with arbitrary large optical depth and arbitrary long propagation distance. Furthermore, our approach allows taking into account non-Lorentzian line shape of the resonance transitions (both one-photon as well as multi-photon). Because the Lorentzian line shape that is typically used in modeling 2PA has far-reaching wings, the choice of actual line shape may strongly influence the outcome of pulse propagation especially if the spectral width of the transitions is broad on the order of 1000 cm^{-1} or more. We address this issue by using stochastic density matrix (SDM) model that has been recently described in [9].

The remainder of this report is organized as follows. In **Section 3** we present theoretical background, which includes a simple analytical solution for plane wave optical power limiting by 2PA, description of the density matrix model of the 2PA chromophores and description of the the step-by-step propagation solution. We also briefly discuss some of the most important technical aspects of the calculation process. In **Section 4** we present results where we study propagation of a Gaussian-shaped incident pulse of 100-fs duration in a three-level 2PA medium modeled after a well-known 2PA absorber. We carry out this calculation for a broad range of input peak intensity 10-10^3 GW/cm^2. We use the calculation data to evaluate the dependence of the nonlinear transmission on the input pulse energy density for various propagation distances in the medium. Finally, in **Section 5** we present conclusions and discuss outlook for future applications.

3. Theoretical background and implementation.

3.1. Simple analytical model of 2PA-based optical power limiting.

Textbook example of incoherent 2PA consists of linearly polarized monochromatic light with intensity that is constant in time. The change of the intensity with the propagation distance, *dz,* may be expressed as:

$$\frac{d}{dz}I(z) = -\frac{1}{2}\sigma_2 n I^2(z), \tag{1}$$

where σ_2 is the molecular 2PA cross section and n is the concentration (number of 2PA chromophore molecules per unit volume). The factor ½ is introduced as a matter of following a previous convention [10]. The differential equation leads immediately to the well-known 2PA attenuation law:

$$I(z) = I_0(1 + \frac{1}{2}\sigma_2 n I_0 z)^{-1}, \quad (2)$$

where I_0 is the incident intensity (number of photons per second per cm^2). As an illustration of equ. (2), let us calculate how the intensity would be attenuated if we assume that the medium comprises trans-4,4'-Bis(diphenylamino)stilbene (BDPAS) molecules whose experimentally measured 2PA spectrum [10] is shown in **Figure 1**.

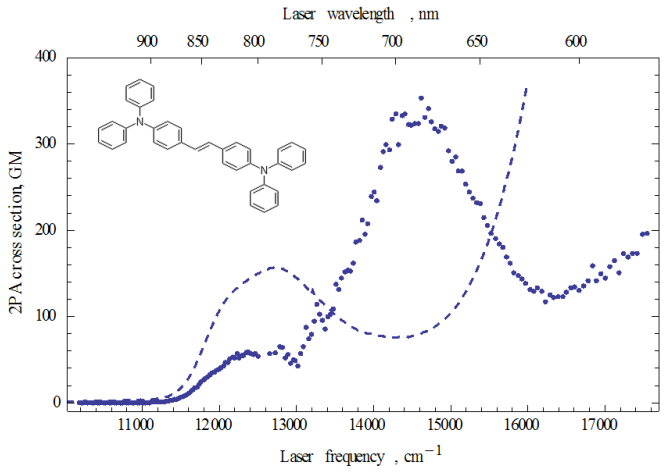

Figure 1. 2PA cross section spectrum (dots) of trans-4,4'-Bis(diphenylamino)stilbene (BDPAS) dissolved in methylene chloride [10]. The spectral shape of one-photon absorption transitions plotted vs twice the normal wavelength is shown for comparison (dashes line). Insert shows the chemical structure of BDPAS.

Suppose that the incident wavelength is 690 nm corresponds to the peak 2PA cross section of BDPAS, σ_2 = 335 GM (1 GM = 10^{-50} cm^4) and that the chromophore concentration is, n=0.5 10^{19} cm^{-3} (8.5 mMol). Left panel of **Figure 2** shows the relative intensity (normalized to the incident intensity) as a function of the propagation distance z (left panel). Right panel of **Figure 2** presents the same data but plotted as a function of the incident intensity for different z values. This simple model predicts, for eample, that for the maximum propagation distance of 0.5 cm the output intensity will be clamped at ~70 GW cm^{-2}.

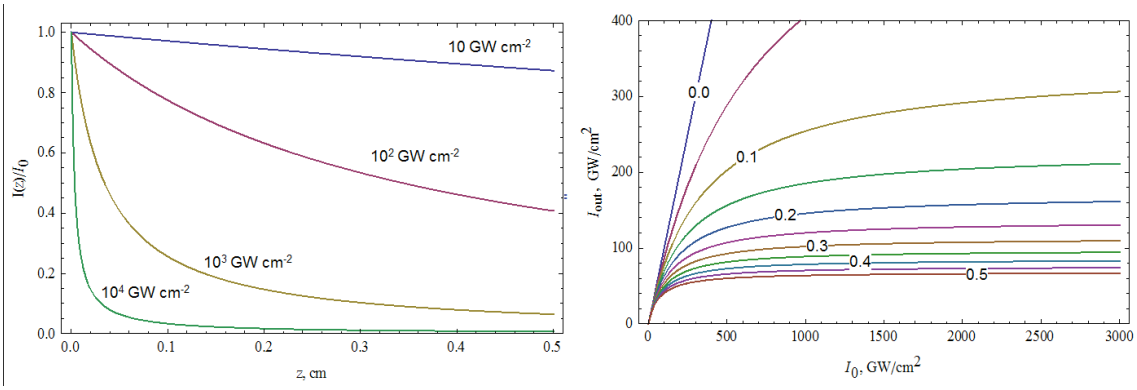

Figure 2. Attenuation of stationary monochromatic light in medium comprising BDPAS molecules at concentration n=0.5 10^{19} cm^{-3}. Left panel – intensity transmission as a function of the propagation distance z for different incident intensity levels; Right panel – clamping of the output intensity for different propagation distances 0 - 0.5 cm.

3.2. Density matrix equation of motion for three-level system.

In our approach the absorbing medium is described by density matrix, $\hat{\rho}$, and the electromagnetic field is given by real-valued oscillating electric field amplitude, $A(t,z)$. The change of the state of the medium with time is obtained by solving the semi-classical quantum-mechanical DM equation of motion:

$$\frac{d}{dt}\hat{\rho}(t) = \frac{1}{i\hbar}[\hat{H}_0 - A(t,z)\hat{\mu}, \hat{\rho}(t)] + \text{relaxation terms}, \tag{3}$$

where $\hat{H}_0$ denotes the unperturbed energy of the molecule and $\hat{\mu}$ is the electric dipole moment operator. For simplicity we are assuming that the optical field is linearly polarized and that all dipole moment vectors are directed in the same direction parallel to the electric field vector. At this stage it is sufficient to consider that the chromophore has maximum of three essential energy levels. In this case the three operators can be written as 3x3 matrixes:

$$\hat{\rho} = \begin{pmatrix} \hat{\rho}_{00} & \hat{\rho}_{01} & \hat{\rho}_{02} \\ \hat{\rho}_{10} & \hat{\rho}_{11} & \hat{\rho}_{12} \\ \hat{\rho}_{20} & \hat{\rho}_{21} & \hat{\rho}_{22} \end{pmatrix}, \quad \hat{\mu} = \begin{pmatrix} \mu_{00} & \mu_{01} & \mu_{02} \\ \mu_{10} & \mu_{11} & \mu_{12} \\ \mu_{20} & \mu_{21} & \mu_{22} \end{pmatrix} \text{ and } \hat{H}_0 = \begin{pmatrix} E_0 & 0 & 0 \\ 0 & E_1 & 0 \\ 0 & 0 & E_2 \end{pmatrix}, \tag{4}$$

of which first two are complex valued and last is real valued. Substituting (4) into (3), and considering the conservation law, $\rho_{00}(t) + \rho_{11}(t) + \rho_{22}(t) = 1$, gives us following set of 8 coupled 1st order ODE:

$$\begin{aligned}
&\frac{d}{dt}Re\rho_{01}(t) = -\gamma_{01}Re\rho_{01}(t) + [A(t)\Delta\mu_{01} - \omega_{10}]Im\rho_{01}(t) + A(t)[Re\mu_{12}Im\rho_{02}(t) + Re\mu_{02}Im\rho_{12}(t) - Im\mu_{12}Re\rho_{02}(t) - Im\mu_{02}Re\rho_{12}(t) + Im\mu_{01}(1-2\rho_{11}(t) - \rho_{22}(t))] \\
&\frac{d}{dt}Im\rho_{01}(t) = -\gamma_{01}Im\rho_{01}(t) - [A(t)\Delta\mu_{01} - \omega_{10}]Re\rho_{01}(t) + A(t)[-Im\mu_{12}Im\rho_{02}(t) + Im\mu_{02}Im\rho_{12}(t) - Re\mu_{12}Re\rho_{02}(t) + Re\mu_{02}Re\rho_{12}(t) - Re\mu_{01}(1-2\rho_{11}(t) - \rho_{22}(t))] \\
&\frac{d}{dt}Re\rho_{02}(t) = -\gamma_{02}Re\rho_{02}(t) + [A(t)\Delta\mu_{02} - \omega_{20}]Im\rho_{02}(t) + A(t)[Re\mu_{12}Im\rho_{01}(t) - Re\mu_{01}Im\rho_{12}(t) + Im\mu_{12}Re\rho_{01}(t) - Im\mu_{01}Re\rho_{12}(t) + Im\mu_{02}(1-\rho_{11}(t) - 2\rho_{22}(t))] \\
&\frac{d}{dt}Im\rho_{02}(t) = -\gamma_{02}Im\rho_{02}(t) - [A(t)\Delta\mu_{02} - \omega_{20}]Re\rho_{02}(t) + A(t)[Im\mu_{12}Im\rho_{01}(t) - Im\mu_{01}Im\rho_{12}(t) - Re\mu_{12}Re\rho_{01}(t) + Re\mu_{01}Re\rho_{12}(t) - Re\mu_{02}(1-\rho_{11}(t) - 2\rho_{22}(t))] \\
&\frac{d}{dt}Re\rho_{12}(t) = -\gamma_{12}Re\rho_{12}(t) + [A(t)\Delta\mu_{12} - \omega_{21}]Im\rho_{12}(t) + A(t)[-Re\mu_{02}Im\rho_{01}(t) - Re\mu_{01}Im\rho_{02}(t) + Im\mu_{02}Re\rho_{01}(t) + Im\mu_{01}Re\rho_{02}(t) + Im\mu_{12}(\rho_{11}(t) - \rho_{22}(t))] \\
&\frac{d}{dt}Im\rho_{12}(t) = -\gamma_{12}Im\rho_{12}(t) - [A(t)\Delta\mu_{12} - \omega_{21}]Re\rho_{12}(t) + A(t)[-Im\mu_{02}Im\rho_{01}(t) + Im\mu_{01}Im\rho_{02}(t) - Re\mu_{02}Re\rho_{01}(t) + Re\mu_{01}Re\rho_{02}(t) - Re\mu_{12}(\rho_{11}(t) - \rho_{22}(t))] \\
&\frac{d}{dt}\rho_{11}(t) = -\Gamma_{10}\rho_{11}(t) + \Gamma_{21}\rho_{22}(t) - 2A(t)[Re\mu_{01}(t)Im\rho_{01}(t) - Re\mu_{12}(t)Im\rho_{12}(t) - Im\mu_{01}(t)Re\rho_{01}(t) + Im\mu_{12}(t)Re\rho_{12}(t)] \\
&\frac{d}{dt}\rho_{22}(t) = -(\Gamma_{21} + \Gamma_{210})\rho_{22}(t) - 2A(t)[Re\mu_{02}(t)Im\rho_{02}(t) - Re\mu_{12}(t)Im\rho_{12}(t) - Im\mu_{02}(t)Re\rho_{02}(t) + Im\mu_{12}(t)Re\rho_{12}(t)]
\end{aligned} \tag{5}$$

Here Γ_{ij} is the population (energy) relaxation rate and $\gamma_{ij}(i \neq j)$ is the rate of decoherence between the levels *i* and *j*. We have also introduced a notation for the transition frequencies: $\omega_{ij} = (\boldsymbol{E_i} - \boldsymbol{E_j})/\hbar$, and for the dipole moments: $\Delta\mu_{ij} = \mu_{jj} - \mu_{ii}$. In the above equations the numerical value of the Planck constant is absorbed in the amplitude *A(t)*. Typical initial conditions for the DM equations is when at *t=0*, i.e. before the arrival of the excitation pulse all matrix elements other than the ground state population are equal to zero:

$$\begin{aligned}
&Re\rho_{01}(0) = Im\rho_{01}(0) = Re\rho_{12}(0) = Im\rho_{12}(0) = Re\rho_{02}(0) = Im\rho_{02}(0) = \rho_{11}(0) = \rho_{22}(0) = 0; \\
&\rho_{00}(0) = 1.
\end{aligned} \tag{6}$$

Not that the rotating wave approximation (RWA) commonly used in solving the nonlinear-optical DM equations is not applicable here. This is because accurate description of 2PA and other essentially multi-photon processes depends on retaining of the higher harmonics created through nonlinear interaction of the oscillation driving field with the molecular system, and which RWA is specifically designed to suppress [11, 12]. For a closely related reason we cannot use the common slowly varying envelope approximation (SWEA), because that would also suppress and distort 2PA in the coherent regime. Nevertheless, numerical solution of (5) (along with the initial conditions) with sufficiently high accurate is quite within the realm of capability of commercial numerical ODE solvers, especially if the applied field does not undergo too many oscillation periods. As will be discussed in more detail below, we are using for this purpose *NDSolve* function of *Mathematica* v.8 package.

A simple example of the excitation pulse is that with carrier frequency, $\omega_p = 2\pi\nu_p = 2\pi c / \lambda_p$ and Gaussian envelope with the duration τ_p (intensity FWHM):

$$A(t) = A_p e^{-\left[\frac{(t-t_p)}{\tau_p 2\ln 2}\right]^2} \cos\omega_p(t-t_p), \qquad (7)$$

where A_p is the pulse peak amplitude and t_p is the pulse peak delay. **Figure 3** shows the normalized amplitude (left panel) and the power spectrum of a pulse (right panel) with the parameter values, τ_p= 100 fs and λ_p= 690 nm. We choose these parameters because for low peak intensities the pulse spectrum may be still considered as nearly monochromatic (compared to the width of the 2PA spectrum), which facilitated comparison between numerical solution and the above simple analytical solution.

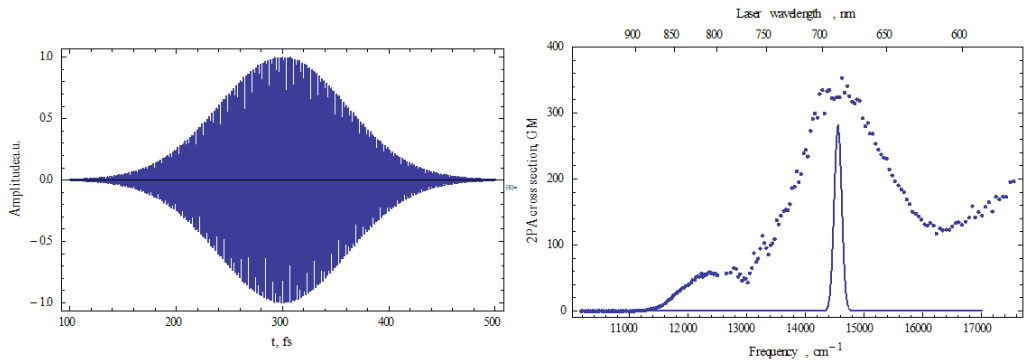

Figure 3. Normalized time domain amplitude (left panel) and the frequency domain power spectrum (right panel) of a pulse with typical the parameter values used in the calculation, τ_p= 100 fs and λ_p= 690 nm. The 2PA spectrum of BDPAS is shown for comparison.

3.3. Simulation of realistic non-Lorentzian line shape.

The phenomenological relaxation introduced in equ. (5) is responsible for finite spectral line widths of the transitions. As the DM is written now, the relaxation is due to the constant decoherence rates, γ_{ij}. Constant relaxation rate that does not depend neither on time or frequency correspond to Markovian process, which leads directly to Lorentzian line shape. Experiment shows, however, that actual line shapes lack the far-reaching "wings" that are characteristic of Lorentzian function. In fact, the real line shapes such as those shown in **Figure 1** are closer to Gaussian (or a superposition of Gaussians). This circumstance is particularly critical for modeling of multi-photon absorption because at the long wavelengths the Lorentzian wing of the 1PA resonance may still be strong enough to interfere with the

2PA transition, which leads to an unrealistic description of the pulse propagation at the 2PA resonance.

We have previously shown that realistic non-Lorentzian line shapes can be modeled by a Monte Carlo type DM calculation, where the transition frequency contains a stochastic component with certain amplitude and frequency distribution [9]. For this we substitute in the equ. (5) the transition frequencies between energy levels *i* and *j* with the following expressions:

$$\omega_{ij} \rightarrow \omega_{ij}[1 + \delta\omega_{ij}\eta_{ij}(t)], \tag{8}$$

where η_{ij}(t) is the stochastic time-domain "noise function" with unit maximum amplitude and $\delta\omega_{ij}$ is the corresponding amplitude. The power spectrum as well as the amplitude of the stochastic "noise function" are adjusted to achieve best correspondence to the measured 1PA and 2PA spectra.

Our next step is to determine molecular parameters for the three-level model that best describe the experimental properties of BDPAS. The corresponding values are shown in **Table 1**. Here and below we assume that transition dipole moments are real valued.

Table 1.

μ_{01}	μ_{02}	μ_{12}	$\Delta\mu_{01}$	$\Delta\mu_{02}$	$\Delta\mu_{12}$	ω_{10}	ω_{20}	$\delta\omega_{10}$	$\delta\omega_{20}$
6.0 D	0	9.0 D	3.4 D	0	0	24800 cm^{-1}	29050 cm^{-1}	0.2	0.27

Figure 4 shows the calculated 1PA and 2PA spectra of BDPAS in comparison to the measured experimental data. Good correspondence is achieved on both linear scale (left panel) and on logarithmic scale (right panel). The quantitative agreement is sufficiently good for current demonstration purposes but could be further improved by fine adjustment of the parameters of the model.

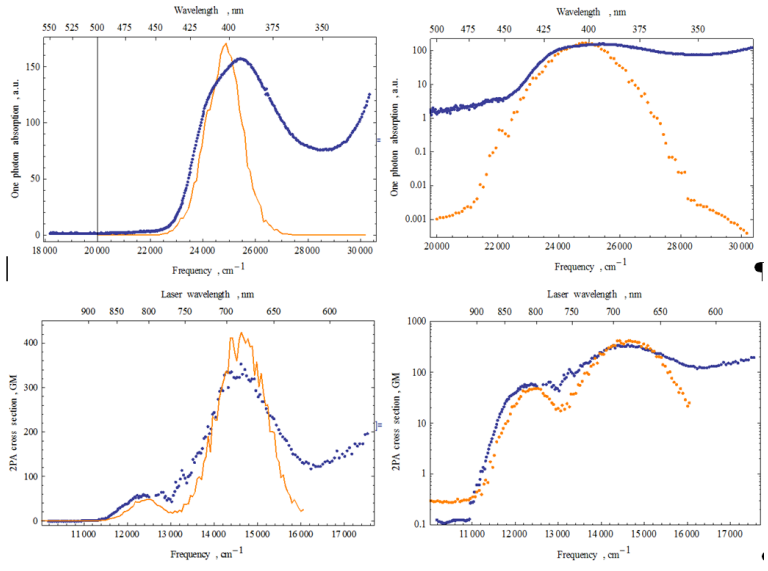

Figure 4. Calculated spectra of BDPAS (orange) compared to the measured experimental data (dark blue); Upper panel - 1PA spectrum; Lower panel - 2PA cross section spectrum. The parameter values used are shown in **Table 1**.

3.4. Step-by-step propagation method.

The task of this project is to develop numerical solutions that describe the propagation of a plane wave front linearly polarized ultrashort light pulse. To address this problem, one typically would needs to solve the DM equations (5) simultaneously with one-dimensional Maxwell's equations:

$$\nabla^2 E(t,z) - \frac{1}{c^2}\frac{\partial^2}{\partial t^2} E(t,z) = \frac{4\pi}{c^2}\frac{\partial^2}{\partial t^2} P(t,z). \tag{9}$$

Here the macroscopic polarization is found from the density matrix:

$$P(t,z) = n\left\langle Tr\,\hat{\mu}\hat{\rho}(t,z)\right\rangle, \tag{10}$$

where the averaging <…> is carried out by integration over an intrinsic sub-wavelength scale distribution of parameters. Typical distribution function $g(\omega,\vec{\Omega})$ describes inhomogeneous spectral shifts of transition frequencies and different orientations of the molecule:

$$\left\langle f(t,z)\right\rangle = \int g(\omega,\vec{\Omega}) f(t,z) d\omega d\vec{\Omega}. \tag{11}$$

Unfortunately, because we cannot take advantage of neither RWA nor SWEA approximations, the exact solution constitutes a rather formidable computational problem. We get around this difficulty by reducing the wave equation (9) to a much simpler case, where reasonable numerical solution is feasible. We note that in complex notation the amplitude of the pulse propagating in vacuum in the positive z direction may be written as follows:

$$\tilde{A}(t,z) = \tilde{A}_p(t - z/c) e^{-i\omega_p(t-z/c)}. \tag{12}$$

The wavy hat (Ã=A% in Mac's rendering, sorry) over the amplitude indicates the analytical signal:

$$\tilde{A}(t) = A(t) + i2Im\int_0^\infty e^{i\omega' t}\int_{-\infty}^{\infty} e^{-i\omega' t'} A(t')\, dt' d\omega', \tag{13}$$

where as before *A(t)* stands for the real amplitude. We use Fast Fourier Transform (FFT) and inverse FFT routines in the *Mathematica* package to implement the calculation of analytical signals equ (13).

Let the pulse be incident at z=0 at 2PA medium consisting of chromophores at a concentration of n molecules per unit volume. The goal is to find the amplitude, $\left|\tilde{A}(t,d)\right|$, and phase, $Arg[\tilde{A}(t,d)]$, of the pulse at the propagation distance *d*.

Let us divide the medium into N thin slices of thickness $\Delta z = d/N$. Each slice will contain only a small number of molecules per unit area, $n\,\Delta z$, such that the polarization (scattering) induced in each slice will have only a small effect on the pulse amplitude. However, with the propagation through many such slices the effect of the induced polarization accumulates, which in turn will result in the attenuation and change of the pulse shape (amplitude and phase). This scheme is illustrated in **Figure 5**, which shows radiation pattern of dipoles excited in the n^{th} layer by the incoming plane wave. The dipole emits coherently in the forward direction. Backward emission (and backward propagation) such as reflection is disregarded. Only coherent emission (scattering) in the forward direction is considered. The amplitude of the incident wave combines coherently with the (much weaker) forward scattering amplitude. The resulting coherent superposition of the two amplitudes creates the input pulse amplitude, which serves as input amplitude for the $(n+1)^{th}$ layer etc.

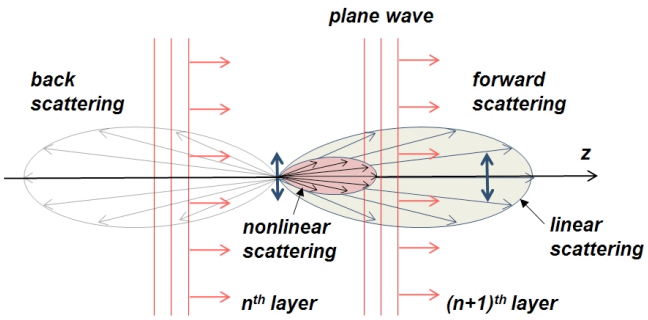

Figure 5. Modified split step method for the pulse propagation in 2PA medium. Incident plane wave travels from left to right. Induced dipole scatters i.e. emits coherently in the forward direction. The scattering consists of linear component and much weaker nonlinear component, where only the last is related to 2PA. Combined amplitude of the incident wave and the scattered wave constitute the input wave for the $(n+1)^{th}$ layer.

The expression for the $(n+1)^{th}$ amplitude is:

$$\mathcal{A}^{n+1}(t) = \mathcal{A}^{n}(t) - \beta \frac{d}{N}\frac{d}{dt}\mathcal{P}^{n}(t). \tag{14}$$

The real polarization is calculated as follows:

$$P^{n}(t) = n2[\mu_{01} Re\rho_{01}(t) + \mu_{02} Re\rho_{02}(t) + \mu_{12} Re\rho_{12}(t)], \tag{15}$$

where the density matrix elements are found by solving the equ. (5) for the n^{th} layer. The constant β represents other factors, such as index of refraction of the medium, orientation of the dipole moments etc. which are not taken into account in this model. The value of β is determined in an empirical manner e.g. by taking the pulse carrier frequency at the peak of the 1PA absorption and then matching the attenuation at low incident pulse intensity with the known linear absorption coefficient and at given chromophore concentration. In addition, in our model we apply spectral filtering of the polarization amplitude and temporal filtering of the pulse amplitude. The spectral filtering is used to eliminate non-physical effects such as second harmonic generation. The temporal filtering is used to cuts off computational artifacts at the start edge and the end edge of the calculated time interval, and which occur because the length of the time interval is finite.

The accuracy of the step-by-step propagation method can be increased by increasing N. However, the nonlinear polarization that is responsible for the 2PA effect constitutes only a small fraction of the overall induced oscillating dipole. Consequently, even at high intensity, most part of the polarization is still due to the one photon resonance, even though the pulse frequency may be detuned far from the 1PA peaks. This means that in reality to achieve reasonable accurately for a practical level of 2PA optical limiting (e.g. 50% or less transmission decrease) the number of the slices N should be quite large, which in turn increases proportionally the calculation time required. We have addressed this issue by solving the DM equation twice for each layer: one time with normal parameters and the second time with the 2PA switched off such that only the 1PA resonances are present. The last is achieved by setting to zero the molecular parameters which are specifically responsible for the 2PA. For example, if we set $\mu_{21}=0$ and $\Delta\mu_{10}=0$, then 2PA vanishes while the "linear" polarization due to the $0 \rightarrow 1$ resonance transition is still present. We subs tract the "linear" polarization from the total (linear + nonlinear) polarization, which gives us the desired 2PA effect but without the large one-photon background. The described method allowed us to substantially increase the maximum absorption per

one layer while maintaining sufficient accuracy for evaluation of optical limiting. This in turn allowed us to decrease the overall number of layers needed N at least by a factor of 10 and accordingly decrease the calculation time.

Another important parameter that factors into the overall calculation time is the number of averages for stochastic DM equation. The simulated spectra (without propagation) presented in **Fig. 4** consists of 120 spectral points, where each represent an average over 280 calculations. The total time for this calculation was about 270 minutes (~4.5 hours) on a 14 core PC, which means that the time needed to solve the stochastic DM for one pulse carrier frequency is about 2 min (up to 10 min if high incident intensity. If we consider that typical number of layers is N= 1000 – 2000 and that solving DM for each layer requires at least 2 minutes, then the overall duration of the calculation would be still prohibitively lengthy. Fortunately, we found a way how to shorten the calculation further. To our pleasant surprise we found that the stochastic averaging works equally well not only if performed separately for each layer, but also if it is performed in the "time forward" direction. From the point of view of smoothing out the stochastic fluctuations in the pulse shape, propagating the pulse through 10 layers has a similar effect as performing the averaging over 10 samples in one layer. The critical condition is of course that the effect of each layer remains relatively small. With this in mind, we found that optimum results in terms of reducing the calculation time versus obtaining a sufficiently smooth pulse shape are achieved if the averaging in each layer is performed about 10-20 time (as opposed to 280 times in **Fig. 4**). This gave us another order of magnitude reduction in the speed of the calculation.

4. Results.

4.1. Verification of the numerical solver by comparison to known analytical solution.

The first objective is to show that at relatively low input intensity the nonlinear transmission corresponds to the simple analytical formula equ.(2). This comparison will allow us to verify if our calculation is indeed delivering qualitatively and quantitatively reliable results. **Figure 6** shows the normalized intensity as a function of the propagation distance for the incident intensity values 47 GW cm^{-2} and 94 GW cm^{-2}. The concentration of BDPAS molecules is n=0.5 10^{19} cm^{-3} in all cases. At these moderate intensities the contribution of saturation should be minimal. Because the spectral width of the 100-fs pulse is several times less than the line width of the 2PA transition, the contribution of coherent effects should be also small. Solid line is the numerical result and the dashed line is the analytical solution. The maximum propagation length is 1 cm, which is divided into N=2000 layers.

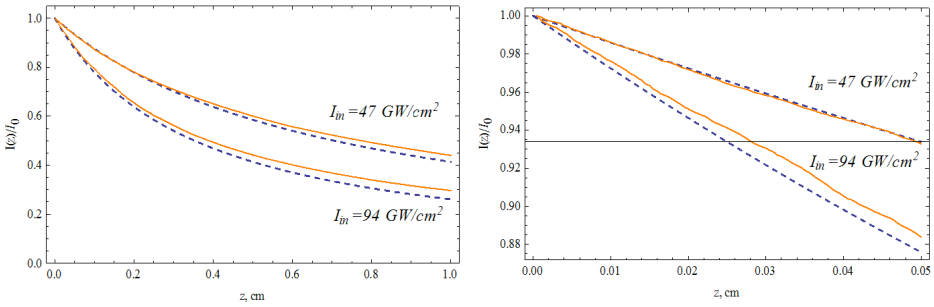

Figure 6. Normalized transmitted intensity calculated numerically (solid line) and analytically (dashed line) plotted as function of the propagation distance for two incident peak intensities 47 GW cm^{-2} and 94 GW cm^{-2}. The medium consists of BDPAS molecules at concentration n=0.5 10^{19} cm^{-3}. The number of layers N=2000 corresponds to the maximum path length 1 cm. Right panel zooms in on the short distance section 0<z<0.05cm.

The fact that our numeric result corresponds well to the analytical result confirms that at least in the low to moderate intensity regime our solver is reliable. The slightly higher transmission for the numerical value is most likely because analytical formula assumes constant intensity. Note that the numerical curves show slight random oscillations or "noise" which is due to the stochastic fluctuations built into the DM equations. It is an interesting observation that the "noise" does not increase with larger z but rather tends to average out. This property is in fact very useful because, as discussed in the previous section, this allows us to reduce the number of averaging steps per each layer. This in turn provides substantial economy in terms of overall computation time.

4.2. Optical clamping and saturation.

As the next step we increase the intensity of the incident pulse, while keeping all other parameters the same. In our case the optical power limiting is accompanied by the change of the pulse shape (see below). However, to facilitate direct comparison to the analytical model shown in **Figure 2,** we assume here that pulse shape does not change, and scale our data considering Gaussian shape (for 100-fs duration Gaussian pulse 1 GW/cm^2 peak intensity corresponds to energy density ~106.4 μJ cm^{-2}). **Figure 7** shows the effective pulse intensity as a function of the incident peak intensity for different propagation propagation distances, z= 0 - 0.5 cm. The data shows that at given concentration n=0.5 10^9 cm^{-3} the minimum propagation distance is, z> 0.4 -0.5 cm. The effective clamping intensity is about 100 GW cm^{-3}, which compares well to the value 70 GW cm^{-3} obtained above for the cw case (dashed curve in **Fig. 7**). On the other hand, if the incident intensity is higher than >10^3 GW cm^{-2}, then the transmission increases again due to the saturation of the absorption.

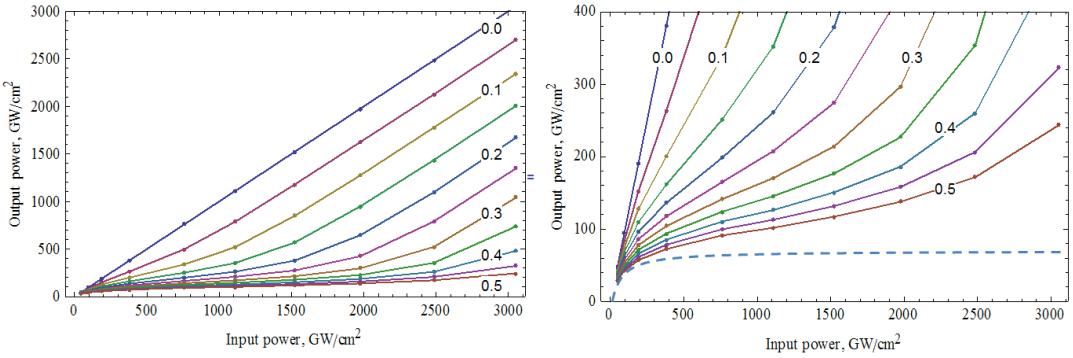

Figure 7. Intensity of 100-fs Gaussian pulse propagating in the 2PA medium (BDPAS at concentration n=0.5 10^{19} cm^{-3}). Left panel – effective pulse peak intensity plotted as the function of the incident intensity for different propagation distances, z = 0 – 0.5 cm. Right panel zooms in on the larger propagation distances showing optical clamping. Dashed curve - data according to the analytical solution for cw light and z=0.5 cm (see Figure 2).

We should mention that at parameter values used here the saturation effects may be also quantitatively described by incoherent rate equations [3,6,7]. We are in the process of performing such comparison calculations to further verify the validity of our new solver. In conclusion of the above section we may say that we have verified that our numerical method indeed works and is able to quantitatively model the performance of realistic optical power limiting media.

4.3. Coherent propagation effects. Time- and spectral domain pulse shaping.

Now we can finally come to the results that show how the propagation changes the temporal shape, the power spectrum of the pulse. We underline that the results presented below are new and can be

obtained only with full DM solution, and cannot be obtained neither with analytical nor with less sophisticated numerical models. **Figure 8** shows the change of the shape of the pulse as a function of propagation distance for two different input peak intensity values. In the case of moderate intensity (47 GW cm^2) the time domain peak diminishes, while the overall shape remains symmetrical. This corresponds to lengthening of the pulse (sometimes called flat-topping). In the spectral domain the shape remains more or less constant; No new frequency components are generated. At higher intensity (250 GW cm^2) substantial change of the temporal and spectral shape occurs. In the time domain, the peak shifts to later times. Most significantly, the peak of the power spectrum shifts to higher frequency. At even higher intensity the spectrum develops oscillation side components.

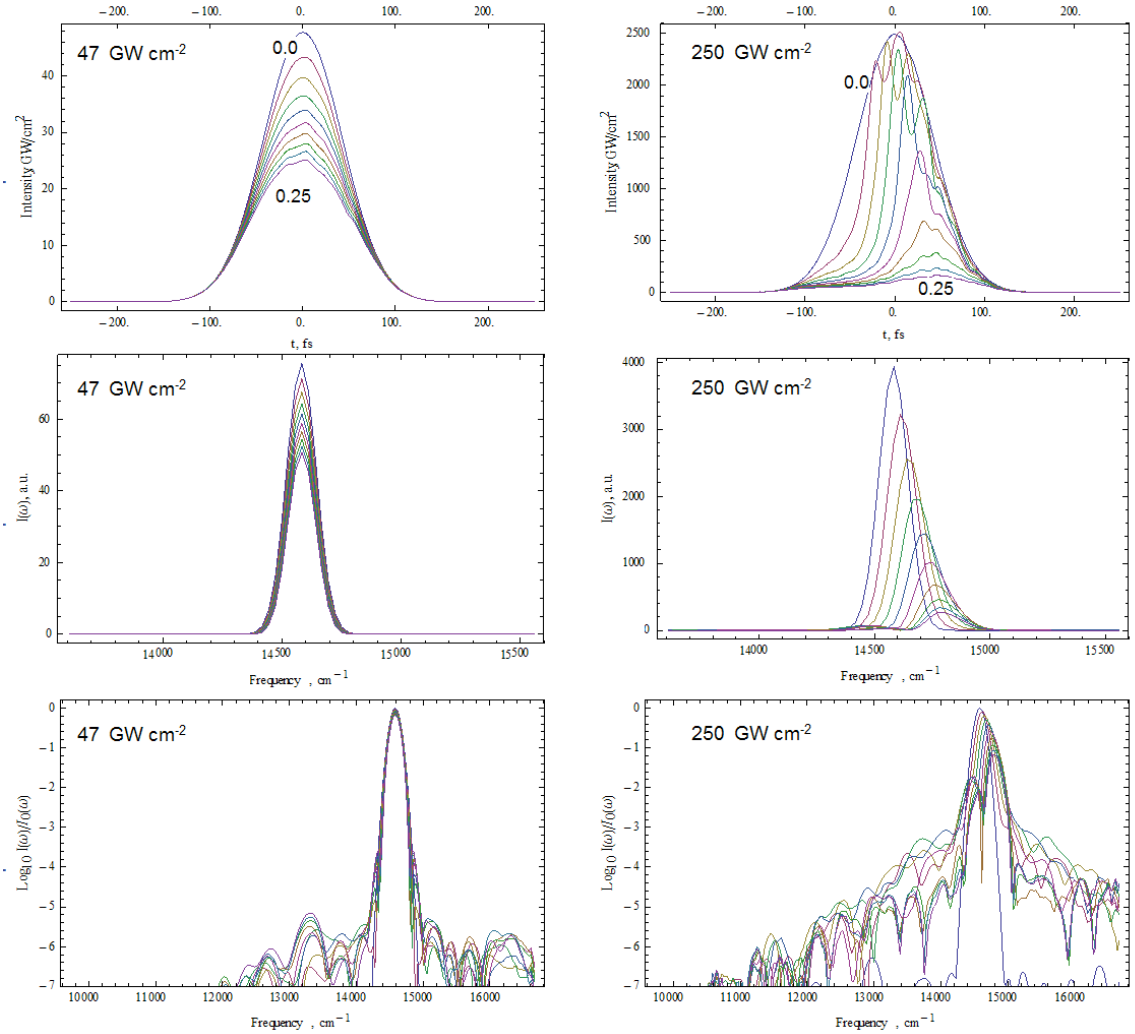

Figure 8. Change of pulse shape as function of propagation distance 0 -0.25 cm for input peak intensity 47 GW cm^2 (left panel) and 250 GW cm^2 (right panel). BDPAS concentration n = 0.5 10^{19} cm^{-3}. Maximum propagation distance z=0.25 cm.

Such characteristic drastic changes of the pulse spectrum propagating in the 2PA medium may have in fact been observed experimentally. **Figure 9** compares our calculated data in BDPAS at concentration n = 0.5 10^{19} cm^{-3} with the measurements performed with 60-fs pulses at 675 nm (estimated peak intensity 4.2 10^4 GW cm^{-3}) below-band-gap propagating through CdS quantum-dot-doped waveguides [13].

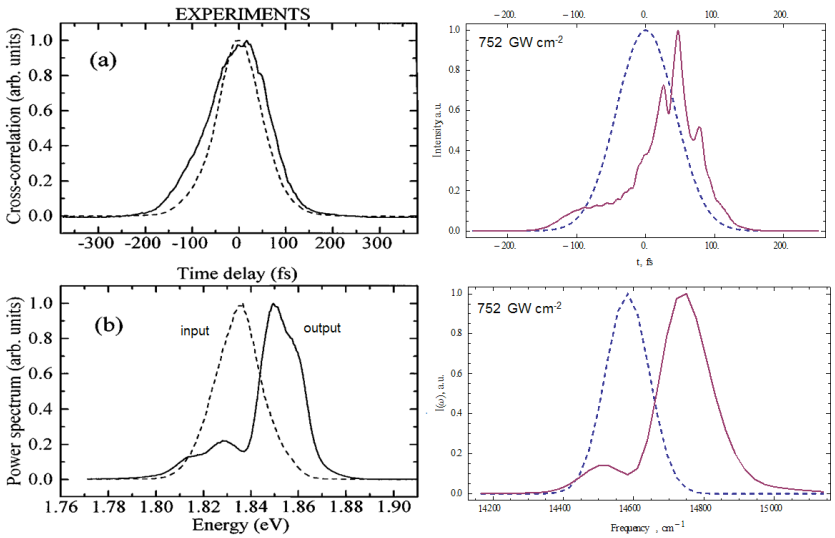

Figure 9. Comparison between calculation and earlier experiments by Guerreiro et al. [13]. The pulse shapes before (dashed) and after (solid) propagation through 2PA medium. Left panel – Time domain pulse cross correlation (upper panel) and power spectrum (lower panel). The experiments were performed in CdS quantum-dot-doped waveguides with 60-fs pulses at estimated peak intensity 4.2 10^4 GW cm^{-3}.

4.4. Nonlinear phase change.

Our calculation allows determining how the phase of the pulse changes with the intensity and the propagation distance. This information can be used to study the effective nonlinear index of refraction caused by the 2PA resonance [14, 15]. Here we mention only one illustration of this possibility leaving more detailed study for the future. **Figure 10** shows the frequency domain phase of 10-fs pulse after propagating through 0.5 cm of BDPAS medium at chromophore concentration n=0.5 10^{19} cm^{-3} for four different input peak intensity values.

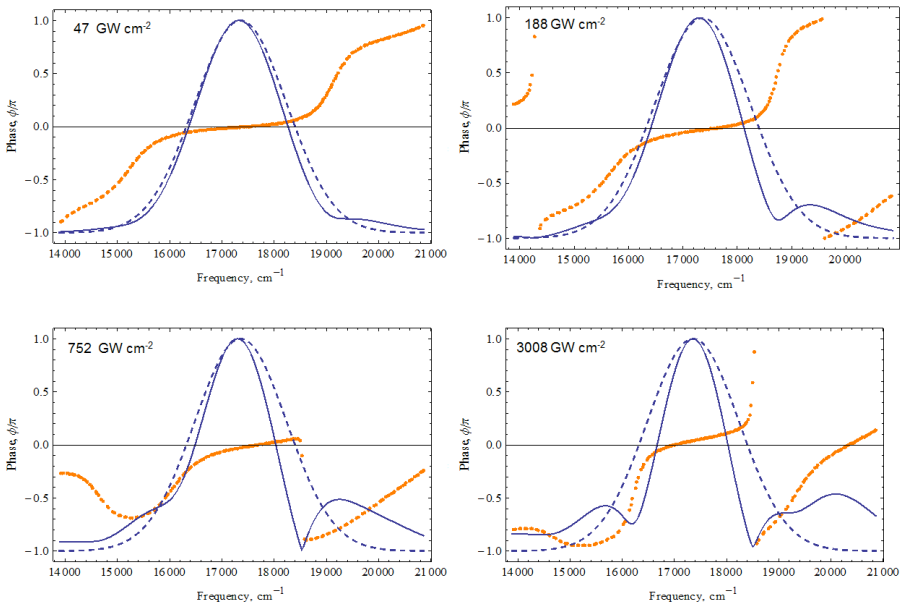

Figure 10. Frequency-domain phase of 10-fs pulse after propagating through 0.5 cm of BDPAS medium at chromophore concentration n=0.5 10^{19} cm^{-3} for input peak intensity values, 47, 188, 752 and 3008 GW cm^{-2}. Orange dots - phase change. Dashed line – spectral amplitude of the incident pulse. Solid line – the spectral amplitude after propagation.

At moderate intensity (upper left panel) the phase change is relatively small and close to constant for all frequency components of the pulse. When the intensity increases, so does the phase change. At the higher intensity (two lower panels) the spectral phase develops a discontinuity (π-jump). The frequency of the phase jump coincides with the frequency where the spectral amplitude changes sign and intensity goes to zero. This behavior is reminiscent of the phase change of soliton amplitude that develop when a coherent pulse propagates in one photon resonance medium. Possibility of formation of solitons in the 2PA resonance medium has been considered previously in [16-18].

5. Conclusions and outlook.

We have developed a versatile numerical technique that allows us to calculate the energy, the temporal shape, the spectrum and the phase of an ultrashort pulse propagating in multi-photon absorbing medium with fully realistic spectral shapes and absorption profiles. Our approach is based on solving straightforward ODE instead of Maxwell-Bloch type equations, which usually require FTDT calculations. Furthermore, our solver is implemented using 100% commercial software (*Mathematica* ver. 8) running on a conventional multi-core PC platform, which avoids complications and increased costs associated with need for custom-produced code and/or large-scale computing facilities. This fact in itself is quite remarkable, especially because we are solving a set of stochastic equations that require extensive averaging. First we verify the accuracy of our calculation by comparing to some simple analytical formulas and then we demonstrate its utility by analyzing the optical power limiting performance of a known two-photon organic chromophore. We also show that the calculation yields full information about the amplitude and phase of the pulse.

Looking forward, we envisage that our new solver can be applied for the simulation and analysis of a broad range of physical problems including coherent- and incoherent regimes of optical power limiting, saturation, CEP effects, soliton formation etc. It can be also used for optimization of materials that are used in multi-photon microscopy and imaging.

6. References

1. D. I. Kovsh, S. Yang, D. J. Hagan, E. W. Van Stryland, "Nonlinear optical beam propagation for optical limiting," *Appl. Opt.* **38** (24) pp. 5168-5180 (1999).
2. E. Gelmukhanov, A.Baev, P. Macak, Y. Luo, H. Agren, "Dynamics of two-photon absorption by molecules and solutions," *J. Opt. Soc. Am. B* **19** (5), pp. 937-945 (2002).
3. R. L. Sutherland, M.C. Brant, J. Heinrichs, J. E. Rogers, J. E. Slagle, D. G. McLean, P.A. Fleitz, *J. Opt. Soc. Am. B* **22** (9), pp. 1939-1948 (2005).
4. A. Baev, P. Salek, F. Gelmukhanov, H. Ågren, "Quantum-classical modeling of nonlinear pulse propagation in a dissolved two-photon active chromophore," *J. Phys. Chem. B* **110**, pp. 5379-5385 (2006).
5. E. Parilov, M.J. Potasek, "Generalized theoretical treatment and numerical method of time-resolved radially dependent laser pulses interacting with multiphoton absorbers," *J. Opt. Soc. Am. B*, **23** (9), pp.1984 – 1909 (2006).
6. Y. Gao, M.J. Potasek, "Effects of excited-state absorption on two-photon absorbing materials," *Appl. Opt.* **45** (11), pp.2521-2528 (2006).
7. S. Gavrilyuk, Ji-Cai Lui, K. Kamada, H. Ågren, F. Gelmukhanov, "Optical limiting for microsecond pulses," *J. Chem. Phys.* **130**, 054114 (2009).
8. Ji-Cai Liu, Chun-Kai Wang, F. Gelmukhanov, "Optical limiting of short laser pulses," *Phys. Rev. A* **76**, 053804 (2007).
9. A. Rebane M. Drobizhev, N. Makaro, E. Beuerman, C. Nacke, J. Pahapill, "Modeling non-Lorentzian two-photon absorption line shape in dipolar chromophores," *J. of Lumin*. **130** (6), 1055-1059 (2010).
10. N. S. Makarov, M. Drobizhev, A. Rebane,"Two-photon absorption standards in the 550-1600 nm excitation wavelength range," *Opt. Exp.* **16** (6), pp. 4029-4047 (2008).
11. A.E. Kondo, V.M. Blokker, W.J. Meath,"Permanent dipole moments and two-color multiphoton resonances in the two-level molecule: The rotating wave approximation versus exact results." *J. Chem. Phys.* **96** (4), pp. 2544-2555 (1992).
12. Ji-Cai Liu, V. C. Felicissimo, F. F. Guimaraes, Chun-Kui Wang, F. Gelmukhanov, "Coherent control of population and pulse propagation beyond rotating wave approximation," *J. Phys. B. At. Mol. Opt. Phys.* **41**, 074016 (2008).
13. P.T. Guerreiro, S.G.Lee, A.S. Rodgigues, Y.Z. Hu, E.M. Wright, S.I. Najafi, J.Mackenzie, N. Peyghambarian, "Femtosecond pulse propagation near two-photon transition in a semiconductor quantum-dot waveguide," *Optics Letters* **21** (9), 659-661 (1996).
14. M. Sheik_Bahae, D.J. Hagan, E.W. Van Stryland, "Dispersion and band-gap scaling of the electronic Kerr effect in solids associated with two-photon absorption," *Phys. Rev. Lett.* **65** (1), pp. 96 – 99 (1990).
15. R. Bavli, Y. B. Band, Nonlinear absorption and dispersion in a two-level system with permanent dipole moments," *Phys. Rev. A*, **43** (9), 5039-5043 (1991).
16. N.P. Garayantz, V.S. Grigoryan, S.A. Michaelian, K.B. Petrossian, K.M. Pokhsrarian, Light-pulse propagation through atomic Cs vapour in conditions of coherent interaction with two-photon absorbing medium," *J. Modern Optics*, **38** (3), pp. 591-595 (1991).
17. A.S. Rodrigues, M. Aantaugustina, E.M. Wright, "Femtosecond pulse propagation and optical solitons in semiconductor-doped glass waveguides in the vicinity of a two-photon resonance," *Opt. & Quant. Electron.* **29**, pp. 961-983 (1997).
18. W. Yang, X. Song, S. Gong, Y. Cheng, and Z. Xu, "Carrier-envelope phase dependence of few-cycle ultrashort laser pulse propagation in a polar molecular medium," *Phys. Rev. Lett.* **99**, 133602 (2007).

7. List of Symbols, Abbreviations and Acronyms

σ_2	*two photon absorption cross section*
μ_{ij}	*electric dipole moment of transition from state i to state j*
$\Delta\mu_{ij}$	*permanet electric dipole moment difference between state i and state j*
2PA	*two photon absorption*
BDPAS	*trans-4,4'-Bis(diphenylamino)stilbene*
SWEA	*slowly varying envelope approximation*
RWA	*rotating wave approximation*
ODE	*ordinary differential equations*
FDTD	*finite difference time domain*
DM	*density matrix*
SDM	*stochastic density matrix*
CEP	*carrier-envelope phase*

8. Appendix
Mathematica program listing.

```
(* Calculate  absorption and  shape of a pulse propagating in  three-level  2PA medium *)
(* Aleks Rebane April 2011. All rights reserved *)
Off[General::"spell1"]
```

```
(* Set directory to write data files *)
ResetDirectory[];
SetDirectory["Rebane/Math/Y2011/Y20110614"];
Directory[];
TableForm[FileNames[]];

(* Check for available kernels  *)
kernels00 = ParallelEvaluate[$KernelID]
kernels01 = {1, 2, 3, 4, 5, 6, 7, 8, 9, 10, 11, 12, 13, 14, 15, 16, 17, 18, 19, 20, 21, 22, 23, 24};
kernels02 = Dimensions[kernels01][[1]];

(* 01. Pulse peak amplitude 20000 esu; Write data to "data_01x.txt" *)
(* Master kernel section *)
(* Define initial distribured functions and parameters *)
noisefilter00 = Table[Exp[-0.0032 * (k - 1)^2] + Exp[-0.0032 * (k - 1202)^2], {k, -1, 1202, 1}];
equ00 := {
    reρ01'[t] == -γ01 * reρ01[t] + (reA0 Δμ01 - ω10) imρ01[t] +
      reA0 (reμ12 imρ02[t] + reμ02 imρ12[t] - imμ12 reρ02[t] - imμ02 reρ12[t] - imμ01 ρ11[t] +
         imμ01 (1 - ρ11[t] - ρ22[t])),
    imρ01'[t] == -γ01 * imρ01[t] + (-reA0 Δμ01 + ω10) reρ01[t] +
      reA0 (-imμ12 imρ02[t] + imμ02 imρ12[t] - reμ12 reρ02[t] + reμ02 reρ12[t] + reμ01 ρ11[t] -
         reμ01 (1 - ρ11[t] - ρ22[t])),
    reρ02'[t] == -γ02 * reρ02[t] + (reA0 Δμ02 - ω20) imρ02[t] +
      reA0 (reμ12 imρ01[t] - reμ01 imρ12[t] + imμ12 reρ01[t] - imμ01 reρ12[t] + imμ02 (1 - ρ11[t] - ρ22[t]) -
         imμ02 ρ22[t]),
    imρ02'[t] == -γ02 * imρ02[t] + (-reA0 Δμ02 + ω20) reρ02[t] +
      reA0 (imμ12 imρ01[t] - imμ01 imρ12[t] - reμ12 reρ01[t] + reμ01 reρ12[t] - reμ02 (1 - ρ11[t] - ρ22[t]) +
         reμ02 ρ22[t]),
    reρ12'[t] == -γ12 * reρ12[t] + (reA0 Δμ12 - ω21) imρ12[t] +
      reA0 (-reμ02 imρ01[t] - reμ01 imρ02[t] + imμ02 reρ01[t] + imμ01 reρ02[t] + imμ12 ρ11[t] - imμ12 ρ22[t]),
    imρ12'[t] == -γ12 * imρ12[t] + (-reA0 Δμ12 + ω21) reρ12[t] +
      reA0 (-imμ02 imρ01[t] + imμ01 imρ02[t] - reμ02 reρ01[t] + reμ01 reρ02[t] - reμ12 ρ11[t] + reμ12 ρ22[t]),
    ρ11'[t] == -γ11 * ρ11[t] + γ22 * ρ22[t] + 2 reA0 (-reμ01 imρ01[t] + reμ12 imρ12[t] + imμ01 reρ01[t] - imμ12 reρ12[t]),
    ρ22'[t] == -γ22 * ρ22[t] + 2 reA0 (-reμ02 imρ02[t] - reμ12 imρ12[t] + imμ02 reρ02[t] + imμ12 reρ12[t]),
    reρ01[0] == 0, imρ01[0] == 0, reρ02[0] == 0, imρ02[0] == 0, reρ12[0] == 0, imρ12[0] == 0, ρ11[0] == 0, ρ22[0] == 0} /.
   ω21 → (ω20 - ω10);
A0 = amp01 * Exp[-((t - t1) * Sqrt[2. * Log[2]] / dt)^2] * Cos[w * (t - t1)];
```

```
para00 = {
    amp01 → 20 000., (* pulse peak amplitude ESU *)
    t1 → 300., (* pulse peak time fs *)
    dt → 100., (* pulse duration fs *)
    tranfreq10 → 24 800. × 2 π * 3. × 10^-5, (* 0→1 frequency cm-1 *)
    tranfreq20 → 29 050. × 2 π * 3. × 10^-5, (* 0→2 frequency cm-1 *)
    w → 14 525 × 2 π * 3. × 10^-5, (* pulse carrier frequency cm-1 *)
    δω10 → 0.2, (* noise amplitude 0→1 transition *)
    δω20 → 0.27 (* noise amplitude 0→2 transition *)
   };
```

```
para01 = {
   (* Transition dipole moments, Debye *)
   reμ01 → (6.0) * 2π * 1.509 × 10^-7,
   imμ01 → 0.,
   reμ12 → (9.0) * 2π * 1.509 × 10^-7,
   imμ12 → 0.,
   reμ02 → 0,
   imμ02 → 0.,
   (* Permanent dipole moments, Debye *)
   Δμ01 → (3.4) * 2π * 1.509 × 10^-7,
   Δμ12 → 0.0,
   Δμ02 → 0.,
   (* Relaxation rates, fs-1 *)
   γ01 → 2π * 0.00001,
   γ12 → 2π * 0.0001,
   γ02 → 2π * 0.0001,
   γ11 → 2π * 0.000001,
   γ22 → 2π * 0.001
  };
  A1 = A0 /. para00;
  equ01 = equ00 /. para01;

  DistributeDefinitions[noisefilter00, equ00, A1, para00, para01, para03];
  (* Parallel evaluation starts using  "kernels01"  *)
  time00 = ParallelEvaluate[TimeUsed[], kernels01];
  (* Create blank data files *)
  energydata01 = Table[0, {k, 1, 1000}];
  pulsedata01 = Table[0, {k, 1, 10}];
  pulsedata02 = Table[0, {k, 1, 10}];
  pulsedata03 = Table[0, {k, 1, 10}];
  pulsedata04 = Table[0, {k, 1, 10}];
  pulsedata05 = Table[0, {k, 1, 10}];
  (* Start k loop; Propagate k layers  *)
  For[k = 0, k < 1000, k++;
    DistributeDefinitions[A1];
    ParallelEvaluate[
     (* Create dummy data files *)
     data00a = Table[0, {t, 0, 1200, 1}];
     data00b = Table[0, {t, 0, 1200, 1}];
     data00c = Table[0, {t, 0, 1200, 0.1}];
     (* Start j loop; Solve ODE j times  *)
 For[j = 1, j < 2, j++;
  noise01a = Table[RandomReal[NormalDistribution[0, 1.0]], {k, -1, 1202, 1}];
  noise02a = Re[InverseFourier[noisefilter00 * Fourier[noise01a]]];
  noisefunca = Interpolation[Table[{k - 1 , noise02a[[k]]}, {k, 1, 1204, 1}]];
  para02a = {ω10 → tranfreq10 * ( 1 + δω10 * noisefunca[t] )};
  noise01b = Table[RandomReal[NormalDistribution[0, 1.0]], {k, -1, 1202, 1}];
  noise02b = Re[InverseFourier[noisefilter00 * Fourier[noise01b]]];
  noisefuncb = Interpolation[Table[{k - 1 , noise02b[[k]]}, {k, 1, 1204, 1}]];
  para02b = {ω20 → tranfreq20 * ( 1 + δω20 * noisefuncb[t] )};
  equ01 = equ00 /. para02a /. para02b /. para00;
  (* Solve ODE with 2PA *)
  equ02 = equ01 /. para00 /. para01 /. reA0 → A1;
  sol01a = NDSolve[equ02, {reρ01[t], imρ01[t], reρ02[t], imρ02[t], reρ12[t], imρ12[t], ρ11[t], ρ22[t]},
     {t, 0, 1200}, MaxSteps → 500 000, AccuracyGoal → 10, PrecisionGoal → 10][[1]];
  (* Repeat the solution of the same ODE with 2PA set to zero *)
  equ01 = equ00 /. para02a /. para02b;
  equ02 = equ01 /. para00 /. para03 /. reA0 → A1;
  sol01b = NDSolve[equ02, {reρ01[t], imρ01[t], reρ02[t], imρ02[t], reρ12[t], imρ12[t], ρ11[t], ρ22[t]},
     {t, 0, 1200}, MaxSteps → 500 000, AccuracyGoal → 10, PrecisionGoal → 10][[1]];
  (* Add up solutions from each run j  *)
  (* Population in the excited states 1 and 2  *)
  datapop11 = (ρ11[t] /. sol01a) - (ρ11[t] /. sol01b);
  datapop22 = (ρ22[t] /. sol01a) - (ρ22[t] /. sol01b);
```

```
    (* Total polarization  *)
    datapol01 =
     (2 (imμ01 * imρ01[t] + imμ02 * imρ02[t] + imμ12 * imρ12[t] + reμ01 * reρ01[t] + reμ02 * reρ02[t] +
           reμ12 * reρ12[t]) /. para01 /. sol01a) -
      (2 (imμ01 * imρ01[t] + imμ02 * imρ02[t] + imμ12 * imρ12[t] + reμ01 * reρ01[t] + reμ02 * reρ02[t] +
           reμ12 * reρ12[t]) /. para03 /. sol01b);
    data01a = Table[datapop11, {t, 0, 1200, 1}];
    data01b = Table[datapop22, {t, 0, 1200, 1}];
    data01c = Table[datapol01, {t, 0, 1200, 0.1}];
    (* Add results of j runs *)
    data00a = data00a + data01a;
    (* data00b=data00b+data01b; *)
    data00c = data00c + data01c
   ],
   (* End  j loop  *)
   kernels01];
  (* End  parallel ODE  *)
  time01 = ParallelEvaluate[TimeUsed[], kernels01];
  Print[k];
  (* Collect  data and average *)
  output01a = Total[ParallelEvaluate[data00a, kernels01]] / 4.;
  output01b = Total[ParallelEvaluate[data00b, kernels01]] / 4.;
  output01c = Total[ParallelEvaluate[data00c, kernels01]] / 4.;
  (* Evaluate Re polarization *)
  repol = output01c;
  (* Remove polarization spectral components outside of the pulse frequency spectrum *)
  complexpolspec = InverseFourier[repol];
  Do[complexpolspec[[i]] = 0, {i, 600, 12001}];
  Do[complexpolspec[[i]] = 0, {i, 1, 300}];
  (* Cut off time-domain artifacts of the complex polarization before and after the pulse *)
  list003 = Fourier[complexpolspec];
  Do[list003[[i]] = 0, {i, 11500, 12001}];
  Do[list003[[i]] = 0, {i, 1, 500}];
  func003 = Table[{0.1 (i - 1), Re[list003[[i]]]}, {i, 1, 12001}];
  func004 = Interpolation[func003][t];
  func005 = D[func004, t];
  complexpol01 = Table[func005, {t, 0, 1200, 0.1}];
  complexpolspec01 = InverseFourier[complexpol01];
  (* Calculate new pulse amplitude *)
  oldpulse01 = Table[A1, {t, 0, 1200, 0.1}];

  oldpulsespec01 = InverseFourier[oldpulse01];
  newpulsespec02 = 2 * oldpulsespec01 - 1. × 10^9 * complexpolspec01;
  newpulsespec03 = newpulsespec02;
  Do[newpulsespec03[[i]] = 0, {i, 600, 12001}];
  Do[newpulsespec03[[i]] = 0, {i, 1, 300}];
  newpulse03 = Fourier[newpulsespec03];
  Do[newpulse03[[i]] = 0, {i, 1, 500}];
  Do[newpulse03[[i]] = 0, {i, 11500, 12001}];
  newpulse04 = Table[{0.1 (i - 1), Re[newpulse03[[i]]]}, {i, 1, 12001}];
  A1 = Interpolation[newpulse04][t];
  (* Save pulse envelope data *)
  (* Print[k]; *)
  energydata01[[k]] = Total[Abs[newpulse03]^2] 10^-11;
  If[
   Element[(k + 99) / 100, Integers],
   l = (k + 99) / 100;
   pulsedata01[[l]] = newpulse03;
   pulsedata02[[l]] = newpulsespec03[[Range[300, 600]]];
   pulsedata03[[l]] = output01a;
   pulsedata04[[l]] = output01b;
   pulsedata05[[l]] = complexpol01
   , 0]
  (* Print[Total[Abs[newpulse03]^2]]; *)
 ]; (* End  k loop  *)
time02 = ParallelEvaluate[TimeUsed[], kernels01];
energydata01 >> data01a.txt; (* Sum of energy of the new pulse *)
pulsedata01 >> data01b.txt; (* complex time amplitude of the new pulse *)
pulsedata02 >> data01c.txt; (* complex spectral amplitude of the new pulse  *)
pulsedata03 >> data01d.txt;  (* dynamics of ρ11 population in time *)
pulsedata04 >> data01e.txt; (*  dynamics of ρ22 population in time *)
pulsedata05 >> data01f.txt; (* Time derivative of spectrally- and time filtered real polarization *)
TableForm[{time01 - time00, time02 - time01} / 60]
```